Original Article

Modeling and analysis of selected organization for economic cooperation and development PKL-3 station blackout experiments using TRACE

Roman Mukin*, Ivor Clifford, Omar Zerkak, Hakim Ferroukhi

Nuclear Energy and Safety Research Division, Laboratory for Reactor Physics and Thermal-Hydraulics, Paul Scherrer Institute, 5232, Villigen, PSI, Switzerland

A B S T R A C T

A series of tests dedicated to station blackout (SBO) accident scenarios have been recently performed at the *Primärkreislauf-Versuchsanlage* (primary coolant loop test facility; PKL) facility in the framework of the OECD/NEA PKL-3 project. These investigations address current safety issues related to beyond design basis accident transients with significant core heat up. This work presents a detailed analysis using the best estimate thermal—hydraulic code TRACE (v5.0 Patch4) of different SBO scenarios conducted at the PKL facility; failures of high- and low-pressure safety injection systems together with steam generator (SG) feedwater supply are considered, thus calling for adequate accident management actions and timely implementation of alternative emergency cooling procedures to prevent core meltdown. The presented analysis evaluates the capability of the applied TRACE model of the PKL facility to correctly capture the sequences of events in the different SBO scenarios, namely the SBO tests H2.1, H2.2 run 1 and H2.2 run 2, including symmetric or asymmetric secondary side depressurization, primary side depressurization, accumulator (ACC) injection in the cold legs and secondary side feeding with mobile pump and/or primary side emergency core coolant injection from the fuel pool cooling pump. This study is focused specifically on the prediction of the core exit temperature, which drives the execution of the most relevant accident management actions. This work presents, in particular, the key improvements made to the TRACE model that helped to improve the code predictions, including the modeling of dynamical heat losses, the nodalization of SGs' heat exchanger tubes and the ACCs. Another relevant aspect of this work is to evaluate how well the model simulations of the three different scenarios qualitatively and quantitatively capture the trends and results exhibited by the actual experiments. For instance, how the number of SGs considered for secondary side depressurization affects the heat transfer from primary side; how the discharge capacity of the pressurizer relief valve affects the dynamics of the transient; how ACC initial pressure and nitrogen release affect the grace time between ACC injection and subsequent core heat up; and how well the alternative feeding modes of the secondary and/or primary side with mobile injection pumps affect core quenching and ensure stable long-term core cooling under controlled boiling conditions.

1. Introduction

The issue of long-term coolability of the core of a nuclear reactor during station blackout (SBO) scenarios has gained further attention following the Fukushima Daiichi disaster. In the framework of the OECD/NEA *Primärkreislauf-Versuchsanlage* (primary coolant loop test facility; PKL) 3 project, the H2 tests series were devoted to the study of beyond-design-basis accidents initiated by an SBO event and resulting in significant core heat up episodes. In

particular, the H2 scenarios were designed to test the effectiveness of different accident management (AM) procedures to avoid a core meltdown and to study the importance of the core exit temperature (CET) signal as a criterion for the initiation and execution of AM procedures. The relevance and suitability of CET in AM procedures is discussed in detail in the study by Tóth et al. [1], and guidelines on how to correctly simulate and reproduce with a thermal—hydraulic model the CET response during a core heat up scenario are proposed in the study by Freixa et al. [2].

Following an SBO event, it can take many hours or even days to restore cooling and bring the reactor to safe shutdown conditions. As

---

a result, in the absence of active cooling, the system temperature, pressure, and coolant mass inventory are determined by core decay power and heat losses. For reactors without passive safety systems, this means that heat losses from components with large outside area, such as the pressurizer (PZR), may play a significant role in the overall system behavior. This effect is increased in an integral test facility (ITF) such as PKL since the surface area to volume ratio of components is considerably larger in a volumetrically scaled-down test facility than in the corresponding full-scale reactor. Thus, one focus of the work presented in the current article is to recall the importance of improving the heat losses model in the case of relatively long transients (more than 10,000 seconds).

In this work, the three SBO tests of the H2 series have been simulated using a single TRACE [3] model of the PKL facility. In the recent years, several other types of tests performed at the PKL facility have been simulated using TRACE at the Paul Scherrer Institute within the Steady-state and Transient Analysis Research for the Swiss reactors (STARS) program [4]. This program aims to address thermal hydraulic safety issues relevant to light-water reactors. The experiments are used for the development and validation of methodologies to simulate the complex phenomena occurring during design and beyond-design basis accidents. Each addition to the PKL tests database not only provides further assessment and improvement of the TRACE model of PKL at hand but also contributes to the improvement of the TRACE models of the actual Swiss reactors.

The three different H2 tests have been designed to evaluate the relevance to the SBO scenario of secondary side (SS) coolant inventory available to secondary side depressurization (SDE), SDE and primary side depressurization (PDE) discharge capacity, accumulator (ACC) behavior, and emergency secondary and primary coolant injection measures. This constitutes an excellent validation basis for the TRACE model of the PKL facility, as it enables us to assess not only how well the model can capture the physical phenomena observed in the tests but also how accurately the timing and relative effectiveness of the different AM measures in reestablishing sustainable core cooling can be predicted. The tests reproduce three scenarios that differ in the initial and boundary conditions. A description of these tests with all AM actions applied during each of the three tests is presented in the Section 2. Section 3 describes the TRACE model used for this validation study, with an emphasis on the key developments made to obtain the level of agreement presented in this article. Namely the improvement of the heat losses model, in particular, to correctly reproduce the conditioning phase and first phase of the three tests, the nodalization of the steam generator (SG) components to better capture

heat transfer as a function of SS water level, and the modeling of the ACCs. In Section 4, the simulation results are analyzed and assessed against the experimental data.

2. H2 tests at PKL

The H2 experimental tests were conducted at PKL, the *Primärkreislauf-Versuchsanlage* (primary coolant loop test facility), in Erlangen, Germany. The PKL is an ITF simulating a 4-loop 1,300 MW pressurized water reactor (PWR) at full scale in height and at scaling 1:145 in volume and power of the reference nuclear power plant (NPP) Philippsburg 2. The facility description and survey of PKL test objectives and programs and some significant results obtained over the years are discussed in studies by Umminger et al. [5–9], with a focus on investigations carried out since the beginning of international cooperation under the auspices of OECD/NEA.

The H2 tests series of the PKL-3 project comprises three different tests and consists of three variants of one scenario initiated by an SBO event. In all the H2 tests, the hypothetical scenarios assume an SBO event that results in the failure of the entire power supply and emergency feedwater power supply systems. The differences between the scenarios are in the initial and boundary conditions of the system, as well as in the AM actions, which are presented for each test in Table 1 in chronological order.

The SBO event first results in the switch off of the main coolant pumps, and natural circulation flow in the primary side is established. Since feedwater becomes unavailable, the SGs' secondary side boils off, leading to the loss of the main heat-sink and subsequent core heat up. Without any operator action, lack of SS heat sink shall result in core uncovery and ultimately in possible core damage. Therefore, the first AM action to ensure core integrity is to initiate an SDE via the main steam relief valves (MSRVs) to resume heat removal from the primary side. As will be shown below, SDE, in this case, has a negligible effect on the primary side, and boiling continues until core uncovery and heat up. According to the test description, at CET > 300°C, the second AM action is PDE via the PZR relief and safety valves. This allows passive coolant injection from ACCs into the primary side. As will be shown, ACC discharge can only temporarily replenish the coolant inventory in the core, as a consequence the second increase in CET is observed. When the CET reaches 300°C again, a mobile pump is used to inject water into the SS of the SG, reestablishing heat transfer from the primary side to the SS. In some of the considered scenarios in which a third CET excursion can be observed, low-pressure emergency core coolant

Table 1
Overview of station blackout AM procedures during H2 tests.

Measure/action		H2.1	H2.2 run 1	H2.2 run 2
1. SDE	Initiation criterion	PZR collapsed water level higher than ~2/3 of PZR height		
	Configuration	2 SGs, 2 MSRV	4 SGs, 1 MSRV of SG 1	4 SGs, 4 MSRV
2. PDE	Initiation criterion	CET > 300°C	CET > 300°C	CET > 300°C
3. PZR valve	Discharge area & rate	100 cm^2/145[a]	143 cm^2/145[a]	143 cm^2/145[*]
	Open/closed after PDE	Open until EOT	Open until EOT	Closed after PDE
	Closing criterion	—	—	T hot legs < 180°C
4. ACC	Configuration	4 ACC cold side (~220 kg per ACC)	4 ACC cold side (~220 kg per ACC)	4 ACC cold side (~220 kg per ACC)
	Actuation pressure	26 bar	26 bar	40 bar
	Nitrogen injection	Yes	No	Yes
5. Sec. feed	Initiation criterion	CET > 300°C	CET > 300°C	CET > 300°C
	Configuration	Mobile pump, 1 × 0.15 kg/s for SG 1	Mobile pump, 1 × 0.15 kg/s for SG 1 and 2	EFWS for 2 SGs (1 & 4) 2 × 0.17 kg/s
6. Primary injection	Initiation criterion	CET > 300°C	CET > 300°C	Not required
	Configuration	1 eRHR-pump, CL 1	1 eRHR-pump, CL 1	
Core power	Configuration	No radial power profile	No radial power profile	Radial power profile

ACC, accumulator; CET, core exit temperature; CL, cold leg; EFWS, emergency feedwater system; EOT, end of test; MSRV, main steam relief valve; NPP, nuclear power plant; PDE, primary side depressurization; PZR, pressurizer; eRHR, Emergency residual heat removal; SDE, secondary side depressurization; SG, steam generator.
[a] 145 is the scaling factor between PKL facility and the reference NPP.

(ECC) injection into the primary side is then necessary to complete the core quench and establish an indefinite core cooling configuration; see AM action 6 in Table 1.

3. PKL facility model description

The original TRACE model of the PKL test facility has been converted from a RELAP5 model developed previously at the Technical University of Catalonia [10]. The pressure vessel (PV) is represented as a set of 1D PIPE components. The core region is modeled as a single pipe with seven axial cells. In the PKL facility, the core simulator comprises 314 electrically heated rods and 26 control rod guide thimbles. The PKL heater rod bundle has a uniform axial power profile and is arranged in three concentric zones that are independently heated to model radially variable power profiles across the test bundle. Inner zone contains 63 rods, intermediate zone 118 rods, and outer zone 133 rods [5]. In the TRACE model, the core heaters are modeled by three different heat structures (one per zone). The four PKL primary loops are symmetrically modeled with 1D PIPE components. In each SG, the U-tube bundle is modeled by one single PIPE component. The SG secondary side is modeled using a TRACE separator component with the two downcomer (DC) pipes modeled using one 1D PIPE component.

In the original TRACE model, the heat losses on the outer surfaces of heat structures were modeled based on a set of constant heat transfer coefficients (HTCs) and outer temperature. This called for a revision of the model to take heat losses more accurately into account in accordance with the reference heat losses determination report for the PKL facility [11]. In addition, the model has been improved by adding fluid power components to more naturally simulate the bypass heaters of the SGs and PZR. The nodalization of the model has also been improved in places, e.g., the nodalization of the primary and secondary sides of the SGs has been improved by introducing finer cells at the bottom of the SGs to more accurately capture the emptying of the SGs. In total, the revised model consists of 463 hydraulic volumes and 1,356 heat structure nodes.

3.1. Modeling of PKL facility heat losses

In TRACE simulations of ITFs (for instance in [12,13]), heat losses can be described by simply applying constant HTC and room temperature on outer surfaces of heat structures. But a unique aspect of typically scaled ITFs, when compared to real power plants, is the relatively large outer surface area to inner hydraulic volume ratio (about 12 times that of the reference PWR in the case of PKL); the surface heat losses are therefore disproportionally high. This is especially relevant in SBO scenarios because these are long transients with periods where active cooling is not available, i.e., passive cooling becomes dominant. Similarly, for another long transient scenario (35,000 seconds) performed at PKL and involving cooldown under asymmetrical natural circulation conditions, it has been observed and analyzed, using ATHLET and CATHARE models, in studies by Salah et al. and Salah and Vlassenbroeck [14,15], that the interruption of natural circulation is sensitive to the cooldown rate of the system, which therefore hints at the need for good characterization of the heat losses as function of the state of the system (e.g., temperature). Also, initial simulations of the H2 tests using the TRACE model assuming constant HTC boundary conditions on the outside surfaces of components such as the PZR gave poor agreement with experimental results. Improved dynamical models for the heat losses have therefore been implemented in this work.

Report by Schollenberger [11] provides detailed measurements of the heat losses in the PKL test facility: the total heat losses, heat losses for individual primary circuit main components, and heat losses for the SS of the SG at different temperatures. Two approaches were used

to determine the heat losses. The first is an integral approach (primary and secondary sides together), taking into account the heat losses either across the whole surface of the complete facility or only across the SS. The second is a separate component approach that was applied only to the primary side of the facility. Heat losses for individual components on the primary side were derived from temperature evolutions recorded during a cooldown transient.

Measured heat losses were converted to heat fluxes of each component and applied independently as a temperature-dependent boundary condition to each heat structure of the TRACE model. In the TRACE model, all system components are represented as cylindrical volumes and cylindrical heat structures, which are attached to the corresponding volumes. Overall, there are 12 different sections of the facility for which heat losses have been measured as a function of temperature. Examples of heat losses in different components, calculated by TRACE during the test H2.2 run 1, are presented in Figs. 1 and 2 as functions of transient time or recasted as functions of component averaged temperature. Red curves in these figures are fits of the heat loss test data and can be considered as our best estimate of the actual heat losses in the facility during the H2 tests.

As can be seen in Figs. 1 and 2, the heat losses depend very much on the components averaged temperature. In all H2 tests the range of surface temperature variation is relatively high for all components. Especially for PZR, parts of the PV, and SGs secondary sides, see Figs. 1 and 2. Such behavior mainly results from the disproportionally increasing heat flux through the insulation material at rising temperature levels and clearly has to be taken into account as a dynamical boundary condition separately for each component.

In Fig. 1A and 1B, examples of heat loss evolution for the test H2.2 run 1 is presented; the black line shows heat losses for the case of constant HTC and outer temperature. An almost constant value of heat loss is predicted during the test. This is particularly important after the start of test (SOT), when the primary pressure is initially dropping due to decreasing core decay heat (following the simulated reactor scram) and then increases again as the water level available for heat removal in the SGs is being boiled off; see Fig. 3. As can be seen, the constant HTC model performed much worse than the new dynamical heat loss model.

3.2. Nodalization of steam generators

After SOT of all H2 tests, water in the SS of the SGs starts to boil off, thus reducing the water level (no SS feedwater systems are available). This gradually affects the heat removal from the primary side. To accurately model the deterioration of heat exchange toward the end of the boil-off phase, the nodalization of the bottom part of the U-tubes and riser has to be more refined; see Fig. 4. In accordance with the TRACE modeling guidance [16], the SG secondary side is modeled as two PIPE components and one separator (SEPD) component. The PIPE components model the DC and boiler region of the SG. The SEPD component is used to represent the SG upper plenum and steam separator. Identical axial nodalization is applied to the boiler region, U-tubes, and heat structures of the SG components to preserve the agreement between local void fraction, i.e., water level in a cell, and corresponding heat transfer efficiency. As seen in Fig. 4, as the water level decreases in the SG the heat exchange also drops since less of water column is available for boiling. Note in the figure the step-wise behavior of the heat exchange power as the water level crosses the elevation of each SG cell interface. This reveals the importance of SG's finer nodalization at the bottom.

3.3. Modeling of accumulators

The TRACE modeling guidance [16] highlights the importance of accurate modeling of ACC volume and the connected discharge line,
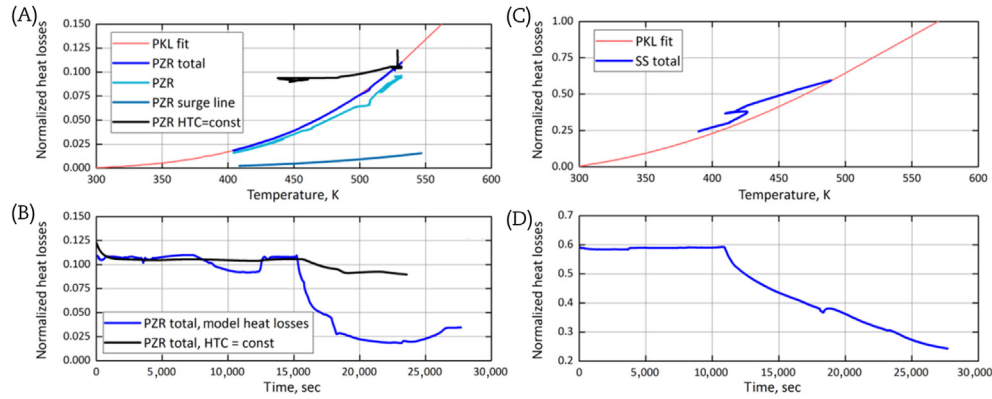
Fig. 1. Normalized heat loss evolution of PZR (A and B) and of the secondary side (C and D). Figures A and C are comparisons with experimental values from [11]. Figures B and D show the corresponding time-evolutions during test H2.2 run 1.
HTC, heat transfer coefficient; PKL, *Primärkreislauf-Versuchsanlage* (primary coolant loop test facility); PZR, pressurizer; SS, secondary side.
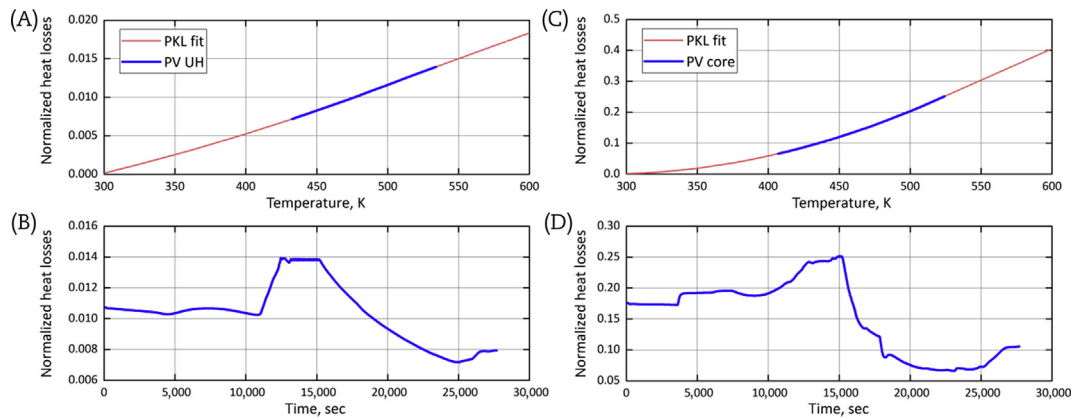

Fig. 2. Normalized heat loss evolution of PV upper head (UH) (A and B) and of PV core (C and D). Figures A and C are a comparison with experimental values from [11]. Figures B and D show the corresponding time-evolutions during test H2.2 run 1.
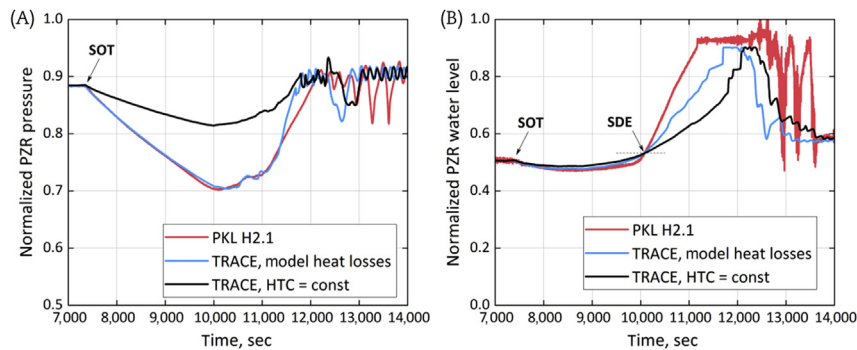PKL, *Primärkreislauf-Versuchsanlage* (primary coolant loop test facility); PV, pressure vessel.

Fig. 3. Normalized pressure and water level evolution in PZR following SOT of H2.1, using constant HTC (black line) and revised heat losses model (blue line).
HTC, heat transfer coefficient; PKL, *Primärkreislauf-Versuchsanlage* (primary coolant loop test facility); PZR, pressurizer; SDE, secondary side depressurization; SOT, start of test.

because the ACCs should serve over a wide range of conditions, from a few seconds during the critical and very dynamic refill phase of a large break loss-of-coolant accident (LOCA) to several hours of intermittent quasi-stationary injection during an SBO scenario. In tests H2.1 and H2.2 run 2, failure of the ACC cut-off valves is postulated, which means that, after emptying of the ACCs, nitrogen enters the reactor cooling system (RCS) via the cold side of the safety injection lines. The nodalization of the ACC and the discharge line is presented in Fig. 5. To model the ACC tank, the TRACE modeling guidance recommends using a PIPE component with modeling option PIPETYPE 1 (Accumulator), 2 (Liquid-separator

model), or 3 (Spherical accumulator model), which all activate a gas/liquid interface sharpener. These options efficiently enable liquid separator models that prevent the gas phase from flowing across the gas/liquid interface. However, it has been observed in simulations of tests H2.1 and H2.2 run 2 using option PIPETYPE 1 that nitrogen can penetrate the discharge line component before the bottom cell of the ACC is empty. As seen from Fig. 5A and 5B, with option PIPETYPE 1, the nitrogen starts penetrating before the ACC empties, and this affects the later behavior of the system. To eliminate this spurious behavior option, PIPETYPE 2 was tested for the ACC PIPE component. This option allows downstream gas flow
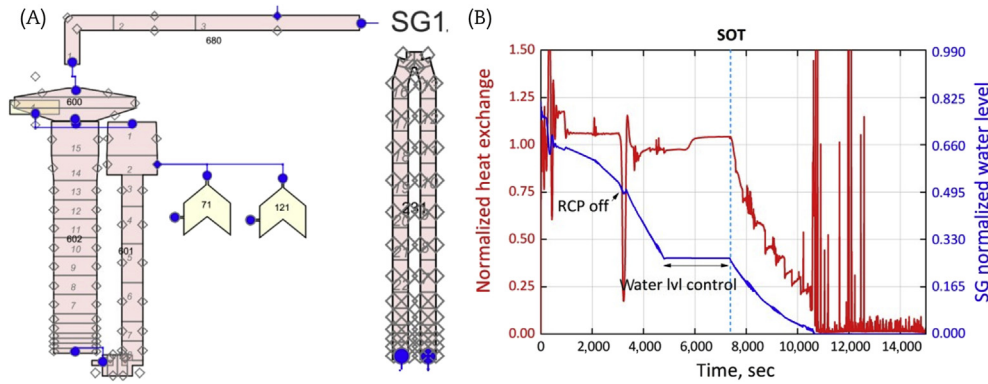
Fig. 4. (A) Nodalization of the SG SS and U-tubes. (B) Calculated and normalized values of heat exchange power and collapsed water level in SG 1 during test H2.1. SOT, start of test; RCP, reactor coolant pump; SG, steam generator.
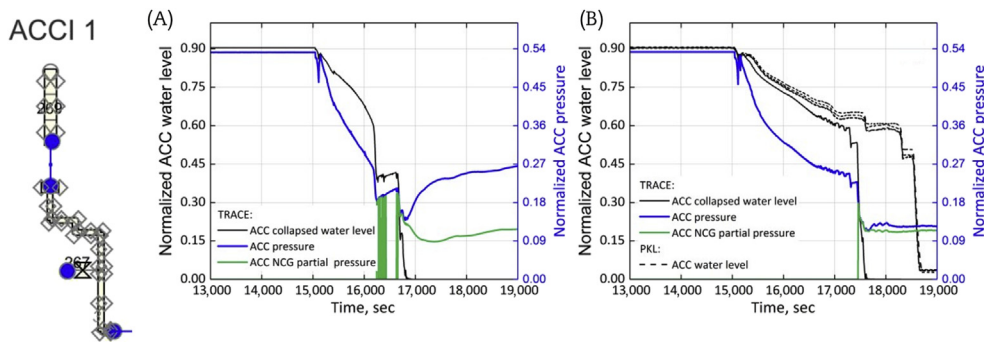

Fig. 5. (A) View of the ACC and discharge line nodalization. (B) Comparison for test H2.1 of the evolutions after ACC discharge signal of normalized collapsed water level, and of total and noncondensable gas (NCG) pressures: (a) for the simulation using option PIPETYPE 1 and (b) for the simulation using option PIPETYPE 2.
ACC, accumulator; PKL, *Primärkreislauf-Versuchsanlage* (primary coolant loop test facility).

only after there is no liquid in the cell. As seen in Fig. 5B, the resulting ACC behavior is more consistent in this case. As a result, the ACC liquid-separator model has therefore been selected for the full analysis of the H2 tests presented in the next section.

4. Simulations of station blackout tests

In this section, simulations and analyses of tests H2.1, H2.2 run 1, and H2.2 run 2 are discussed. All tests are divided into four consecutive phases: conditioning, phase A, phase B, and phase C. The first two phases, conditioning and phase A, follow the same sequence of events and, therefore, discussions for these phases are presented together for all tests in the next subsections. Phases B and C assume different variants in the AM procedures and configurations of safety systems; see Table 1. Therefore, results and analysis for these phases are presented for each test in separate sub-sections.

4.1. Conditioning phase and phase A

The conditioning phase serves to set up initial conditions of the facility before the SBO scenario starts. For all tests, the same sequence of events was performed. Simulation results for test H2.1 are presented in Figs. 6 and 7. This phase started with completely filled PV and SGs and a half-filled PZR. The core power was commensurate with PWR zero-load condition, i.e., constant 3.5% power level, with additional compensation for the heat losses. The reactor coolant pumps (RCPs), chemical and volume control system (CVCS) for PZR level control, and SG's feedwater and main steam systems, initially in operation, were sequentially switched off during the conditioning phase. First, the SG's feedwater system was terminated, which led to water boil-off in the SGs and venting via the SG relief valve (RV), thus

controlling the secondary pressure at around 21.5 bars. In the TRACE model, this is simulated by adjusting the position of the RV and the SG bypass heater power, using control logic information provided by the PKL-3 project. After the water level in the SGs dropped to a certain value, the RCPs were switched off and a transition to natural circulation was observed; see Fig. 6. As can be seen, the coolant circulation flow rate became much smaller. As a consequence, the coolant temperature in the primary side increased because core power remained constant. To compensate for coolant thermal expansion on the primary side, the CVCS system was applied, as can be seen in the PZR water level evolution shown in Fig. 7. During these
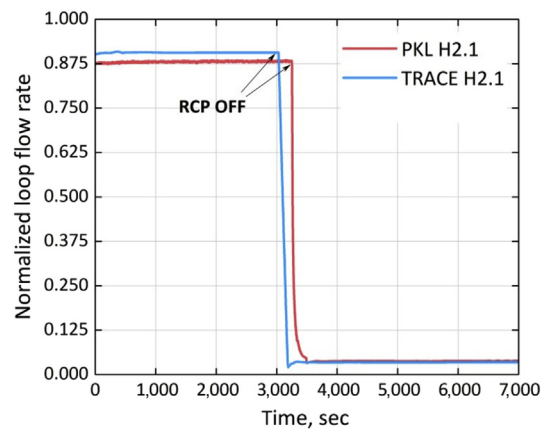

Fig. 6. Normalized loop flow rate evolution during conditioning phase.
PKL, *Primärkreislauf-Versuchsanlage* (primary coolant loop test facility); RCP, reactor coolant pump.
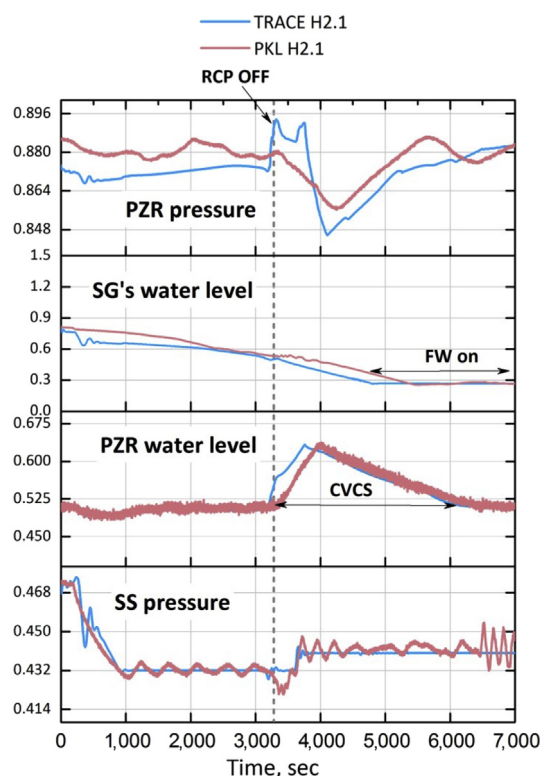
Fig. 7. Normalized main parameter evolution during conditioning phase.
CVCS, chemical and volume control system; PZR, pressurizer; RCP, reactor coolant pump; SG, steam generator; SS, secondary side.

events on the primary side, water boil-off continued in the SS and, by the end of the conditioning phase, the feedwater system was reactivated in all SGs to maintain a constant water level until the SOT.

Although the conditioning procedure was the same in all the tests, the initial targeted conditions were not identical, in particular the primary pressure. Stationary results at the time of SOT obtained

by the TRACE model are compared with the corresponding measured values in Table 2. As can be seen in the table, the primary side pressure and CET in tests H2.2 were higher than in test H2.1. Also, SG4 had a higher water level than the other SGs in tests H2.2, due to systematic error during the test. Consequently, heat exchange via SG4 should last longer compared to the other SGs. Water level and temperatures in the ACCs were also higher in tests H2.2 than in test H2.1.

The actual SBO event was initiated at the beginning of phase A or SOT by switching off the CVCS, SG's feedwater system, and PZR bypass heater and by actuation of core power decay to simulate reactor scram. Since the SGs were partly filled at SOT, heat exchange between primary and secondary sides was enough to remove decay heat from the core. Therefore, primary pressure and CET started to decrease after SOT. As a result of water boil-off and corresponding level depletion in the secondary side of the SGs, the primary/secondary heat exchange gradually dropped. At 3,250 seconds from SOT, following tripping of the RCPs, the heat sink was no longer sufficient to take away all the heat generated in the core; as a consequence, the CET started to increase, thus causing a water level rise in the PZR. When the water level in the SGs became zero, heat exchange between the sides was completely lost. The CET, therefore, started to rise faster and when the temperature reached saturation conditions boiling started in the core and caused the formation of a void in the upper head (UH) of the PV. Void formation in the PV accelerated the rising of the PZR water level since water from PV was pushed out into the primary loops by the void formed in UH; see PZR water level evolution in Fig. 8.

According to emergency operation procedures, SDE is the preferred measure for restoring heat removal from the primary side, before having to resort to fast cooldown via the PZR relief valve (PZR-RV). Also, in the hypothetical scenarios considered in the H2 tests, emergency water feeding of the SGs by a mobile pump was arbitrarily delayed and initiated only after ACC discharge became ineffective in cooling the core. In the H2 tests, the SDE was actuated when the PZR was two-thirds full of coolant. Since the SGs were empty at that time, SDE did not affect the primary side. So, the primary side continued to heat up, i.e., CET, primary pressure and water level in the PZR continued to rise; see Fig. 8.

Table 2
Comparison of measured and calculated tests initial conditions after conditioning phase (all values are normalized to an arbitrary maximum value of a corresponding parameter).

Parameter	H2.1		H2.2 run 1		H2.2 run 2	
	PKL	TRACE	PKL	TRACE	PKL	TRACE
Primary pressure						
Upper plenum	0.892	0.891	0.935	0.940	0.940	0.941
PZR	0.883	0.882	0.933	0.943	0.932	0.933
Pressurizer						
Inventory	—	0.450	—	0.446	0.450	0.450
Temperature (liq.)	0.854	0.857	0.863	0.862	0.864	0.868
Level	0.504	0.507	0.513	0.500	0.511	0.508
Loop Flows						
Loop 1/2	0.0380/0.0375	0.0345/0.0348	0.0381/0.0375	0.0347	0.0373/0.0365	0.0348/0.0348
Loop 3/4	0.0360/0.0378	0.0348/0.0345	0.0368/0.0380		0.0353/0.0380	0.0345/0.0348
RCS Temperatures						
CET	0.500	0.500	0.508	0.500	0.509	0.500
UH	0.493	0.428	—	0.402	—	0.428
Secondary side						
Pressure SG 1/2	0.440/0.446	0.440/0.440	0.434	0.440/0.440	0.424/0.434	0.440/0.440
Pressure SG 3/4	0.448/0.442	0.440/0.440		0.440/0.440	0.436/0.424	0.440/0.440
Water level SG 1/2	0.267/0.275	0.267/0.277	0.273/0.273	0.274/0.274	0.280/0.273	0.280/0.274
Water level SG 3/4	0.276/0.275	0.280/0.274	0.273/0.283	0.274/0.281	0.280/0.327	0.274/0.328
ACC						
Pressure ACC 1/2	0.524/0.518	0.533	0.52	0.52	0.802/0.802	0.802/0.802
Pressure ACC 3/4	0.520/0.520				0.802/0.800	0.802/0.800
Water level ACC 1/2/3/4	0.90	0.90	0.97	0.97	0.94	0.94
Temp. bot ACC 1/2	0.860/0.763	0.833	0.92	0.92	1.027/0.960	1.027/0.960
Temp. bot ACC 3/4	0.770/0.837				0.920/1.000	0.920/1.000

ACC, accumulator; CET, core exit temperature; PKL, *Primärkreislauf-Versuchsanlage* (primary coolant loop test facility); PZR, pressurizer; RCS, reactor cooling system; SG, steam generator; UH, upper head.
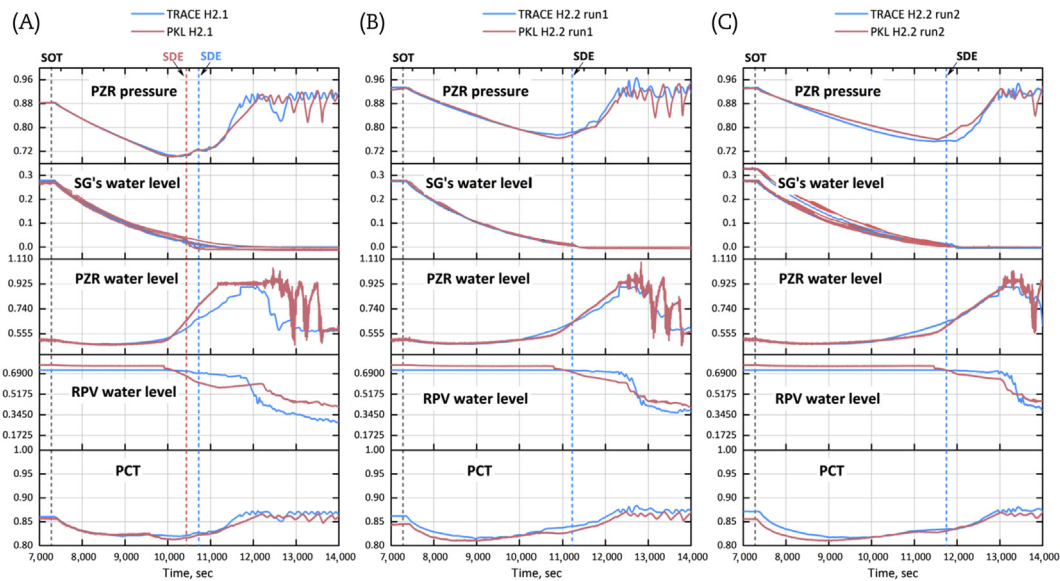
Fig. 8. Comparison of normalized main parameters evolution during phase A for SBO tests. (A) H2.1. (B) H2.2 run 1. (C) H2.2 run 2.
PCT, peak cladding temperature; PZR, pressurizer; SDE, secondary side depressurization; SG, steam generator; SOT, start of test.

To prevent further increase of the primary pressure, the PZR safety valve (PZR-SV) started to operate at the end of phase A. This led to substantial inventory loss through steam venting increase via void formation in the PV. Liquid started to drain from the SG U-tubes when the PV water level dropped to the elevation of the hot legs, resulting in loop seal formation, thus stopping natural circulation in the system.

After the water level in the PV dropped to approximately half of the core height, the core started to heat up. AM procedures were therefore initiated in phases B and C, described in the subsections below, to restore coolant inventory and to cool the primary side.

During the conditioning phase and phase A, passive heat losses played an important role. For instance, the slight difference in peak cladding temperature (PCT) from the measured values at SOT in tests H2.2 run 1 and run 2 (around 3°C) could be eliminated by slightly adjusting the heat losses of the PV. But this type of test-dependent and local adjustment approach has not been retained, and an identical dynamical heat losses model has been applied for all H2 tests to ensure consistency in the validation approach. One can, however, note that dynamical heat losses for all components have been obtained for the quasi-stationary state, natural circulation at relatively low-pressure conditions and fixed water levels in all components, which could introduce some uncertainties in the heat losses model when applied to nonstationary conditions such as the ones experienced in H2 tests. As we saw in all the tests, the pressure was often higher than that considered for the heat loss characterization in [11], and the water level in all components changed quite significantly: for instance, the water level in the PZR evolved from low to completely full and back to nearly empty.

Nevertheless, after SOT, the model showed good agreement with the measured evolutions of pressure (primary and secondary sides), collapsed water levels and temperature, which resulted from core power decay and gradual degradation of the heat sink from the SS as a function of water boil-off in the initially filled SGs. This correct behavior was made possible thanks to the more accurate dynamical heat loss model applied to the system components and to the refined nodalization of the SG components. The scenarios continued with the gradual loss of the heat exchange between primary and secondary sides, thus resulting in coolant expansion and displacement

from PV to PZR due to boiling in PV and void formation in UH of PV, which expelled coolant from the hot leg to the PZR. The rising of the water level in the PZR was captured by the TRACE model but appeared slower than what data showed for all the H2 tests. Therefore, the first AM execution, i.e., SDE, was often predicted later than in the actual tests.

Both the H2 tests and corresponding model results showed the ineffectiveness of SDE for primary side heat removal. As a consequence, the primary pressure continued to rise to the point where pressure started to be limited by PZR-SV with intermittent but substantial primary inventory loss for approximately 500 seconds. In the model, the inventory loss was larger than in the H2 tests; see Figs. 10–12. This significantly anticipated the point of core uncovery and therefore the time of initiation of the next AM action, namely the PDE, which occurred earlier in the model.

4.2. SBO test H2.1

Phase B in test H2.1 started with the initiation of PDE when CET > 300°C; see Table 1. In test H2.1, PZR-SV had a flow limiting cross-section of 100 cm²/145. As can be seen in Fig. 10 the simulated inventory loss during pressure blowdown via PZR-SV is larger than that observed from PKL measurements and mass flow rate from PZR-SV showing substantial liquid flow rate, since PZR was completely filled with water at the beginning of pressure control via PZR-SV. A substantial amount of coolant release via PZR-SV is predicted leading to earlier core uncovery and rising of the CET and PCT signals. According to the specifications for this test, ACC injection to the cold legs (CLs) is activated when the primary pressure drops to half of the nominal pressure. As a result, loop-seal clearing effect is observed in this case, and the pressure between hot and CLs is equalized. Owing to the design of the ECC line, which is inclined towards the PV, the injected water streamed preferentially to the DC and core, initiating quenching.

In test H2.1, ACC injection proved not sufficient for complete core quenching. The TRACE model, however, predicted full quenching of the core, as can be seen in Fig. 9. The PCT and CET signals are affected by ACC injection much faster in the TRACE simulations than in PKL measurements. One possible explanation for this behavior in TRACE could be related to the modeling of the
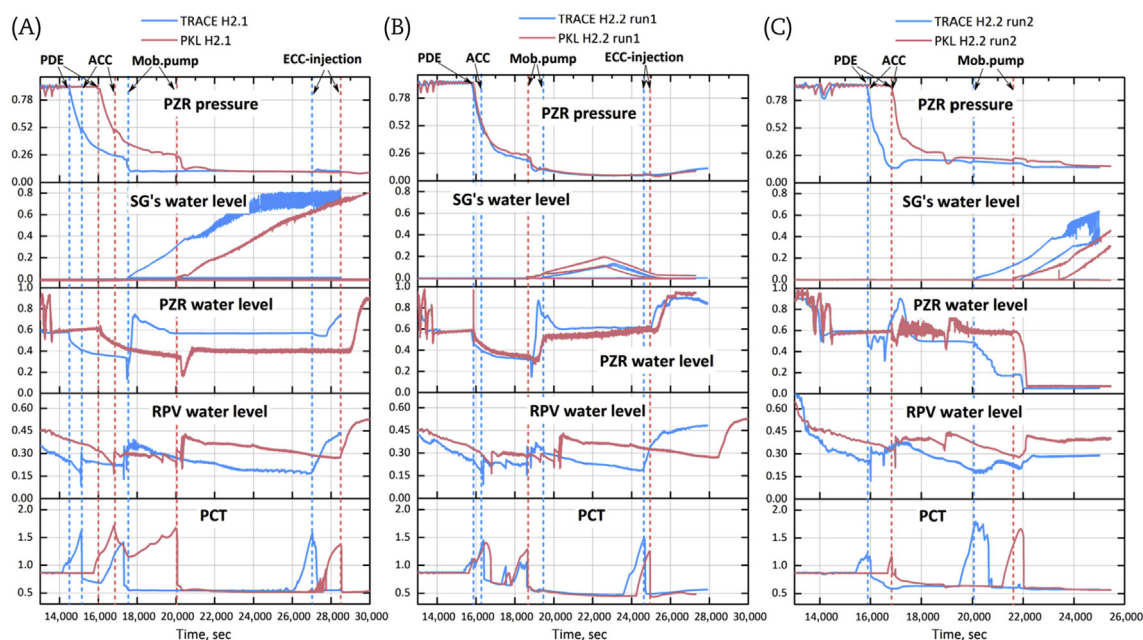
Fig. 9. Comparison of normalized main parameters evolution during phases B and C for SBO tests. (A) H2.1. (B) H2.2 run 1. (C) H2.2 run 2.
ACC, accumulator; ECC, emergency core coolant; PCT, peak cladding temperature; PDE, primary side depressurization; PZR, pressurizer; RPV, reactor pressure vessel; SG, steam generator.

ACC injection line, although the predicted general behavior of the ACC seems in reasonably good agreement with the H2.1 data; see Fig. 5. One can also notice that the modeled PCT excursions start earlier and at a slightly lower PV water level indication, compared to what the data showed. The predicted onset of PCT excursion at a lower PV water level could hint at the need to represent more precisely the hydraulic volume distribution within the core and the PV in the current model. After pressure equalization in ACC and on the primary side, the coolant inventory in the core continued to drop, and the PCT and CET temperatures started to rise again.

Phase C starts with the feeding of the SS of SG1 with the mobile pump when CET > 300°C to prevent core overheating. The objective of this procedure is to resume heat removal via SG1. This action induces steam condensation on the primary side of the U-tubes of SG1 and a decrease of the primary pressure, allowing for further slow and continuous ACC discharge. However, after ACC eventually emptied, nitrogen started to penetrate the primary system. The noncondensable gas accumulated in the upper part of the SG1 U-tubes and reduced heat removal efficiency there. Since the PZR-RV remained open, continuous inventory loss on the primary side led to further increase in temperatures in the core upper part. Since the primary pressure at this stage was relatively low, low-pressure safety injection (LPSI) could be activated using the emergency fuel pool cooling pump (FPCP). Thus, when CET crossed 300°C, LPSI injection into CL1 was initiated. The injection rate was sufficient to ensure continuous core cooling and eventually to fully quench the core and prevent further steam accumulation on the primary side.

4.3. SBO test H2.2 run 1

Similar to the previous test, PDE in test H2.2 run 1 was also initiated at CET > 300°C (see Table 1), but the PZR-RV had a valve cross-section larger than in H2.1, which provided additional mass and heat sink via PZR-RV. Together with the increase of water level swell in the core during the pressure blowdown, a cooling effect was observed, which only delayed the core heat up, since inventory was continuously lost via PZR-RV leading to core uncovery. Similar to test H2.1, ECC injection from the four ACCs is initiated. Loop-seal

clearing similarly occurs, induced by the suction effect of ACC injection in the CLs. In contrast to test H2.1, a complete quench of the core was observed in this case, and the PCT evolution predicted by the model more closely matches the experimental results (see PCT temperature evolution in Fig. 9), although these heat up and quench episodes again take place at different PV level indications, as this was already noted for test H2.1. Only around 20% of ACC coolant inventory was injected into the system at this stage. However, since the PZR-RV remained open and primary side inventory loss continued, a second core heat up occurred at 17,300 seconds. Complete core quenching in this test can be related to the larger steam venting capacity via PZR-RV than that in test H2.1. Beginning of ACC injection delayed the core heat up, and when CET reached 300°C, SS feed to SG1 and SG2 using mobile pumps was initiated. As discussed earlier, SS feed reactivates the heat transfer from the primary to the secondary side. This action initiates the primary pressure reduction due to condensation in the SGs U-tubes and continuation of ACC injection. Second ACC injection due to condensation in CLs creates loop-seal clearing condition anew. In addition, condensation on the CL injection points intensifies ACC injection, leading to the displacement of coolant into the PV DC and further to the core. After ACC injection has been completed, ACC cut-off valves operated correctly, thus preventing nitrogen injection into the system, and hence there was no adverse effect on the heat exchange between the primary and secondary sides. At this stage, three heat sinks were available, via SG1, SG2, and PZR-RV. The primary coolant inventory evolution (see Fig. 10) shows a steady decrease, since the flow rate via PZR-RV is rather small. To shorten the test, the mobile pump was stopped after 500 seconds of operation, leading to a decrease of the water level in the SSs of SG1 and SG2 and reducing the heat transfer to the SS. During mobile pump operation, the primary pressure decreased to the low-pressure range at which LPSI became possible via FPCP injection. At 24,200 seconds in the actual test and 23,500 seconds in the model simulation, a third core heat up episode was observed, again at visibly different PV water level indications (see Fig. 9). Low primary pressure however allowed efficient application of FPCP injection, which led to rapid core quench and long term core cooling.
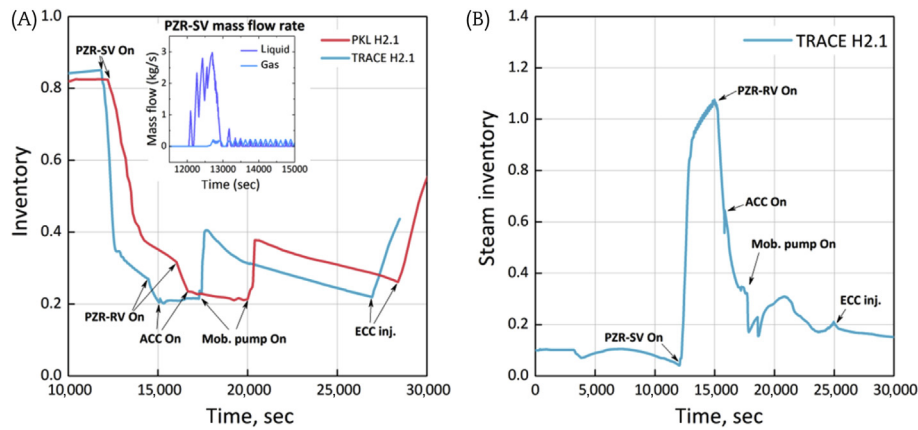
Fig. 10. Test H2.1. (A) Normalized primary inventory evolution in test H2.1. (B) Primary steam inventory evolution in test H2.1.
ACC, accumulator; ECC, emergency core coolant; PZR-RV, PZR relief valve; PZR-SV, PZR safety valve.
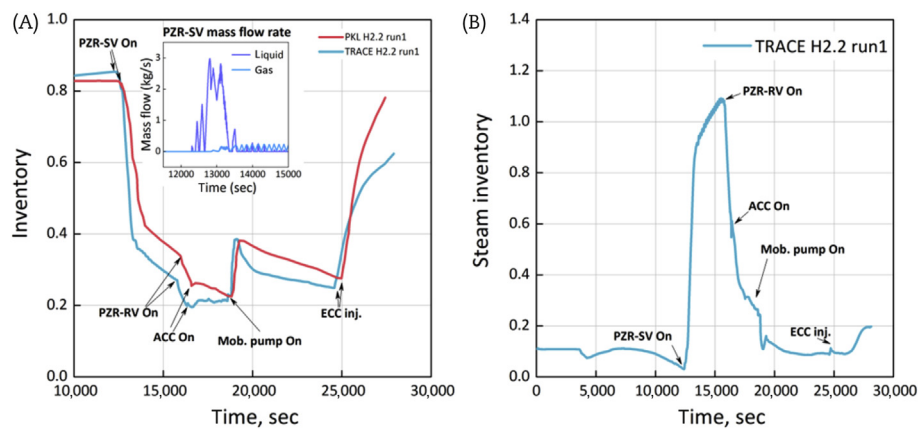

Fig. 11. Test H2.2 run 1. (A) Normalized primary inventory evolution in test H2.2 run 1. (B) Primary steam inventory evolution in test H2.2 run 1.
ACC, accumulator; ECC, emergency core coolant; PZR-RV, PZR relief valve; PZR-SV, PZR safety valve.

4.4. SBO test H2.2 run 2

Before discussing phases B and C, one should recall a first difference between H2.2 run 1 and H2.2 run 2 that was already present in phase A. Indeed, not only was the SDE done in phase A of run 2 via all four MSRVs of the SGs, but the initial SS water inventory at time of SOT was slightly larger in run 2 than in run 1 (see the SGs water levels in Table 2). This means that, in run 2, the heat sink

capacity via SS was more significant than in the previous scenarios. This had an impact on the timing of the PZR water level increase during phase A (see Fig. 8), an effect that the TRACE model was able to capture reasonably well.

As for phase B, PDE and primary pressure control actions started much earlier in the TRACE model simulations, compared to what was observed during the PKL test. The discrepancy in the timing of events is more significant than for test H2.2 run 1 and more in line
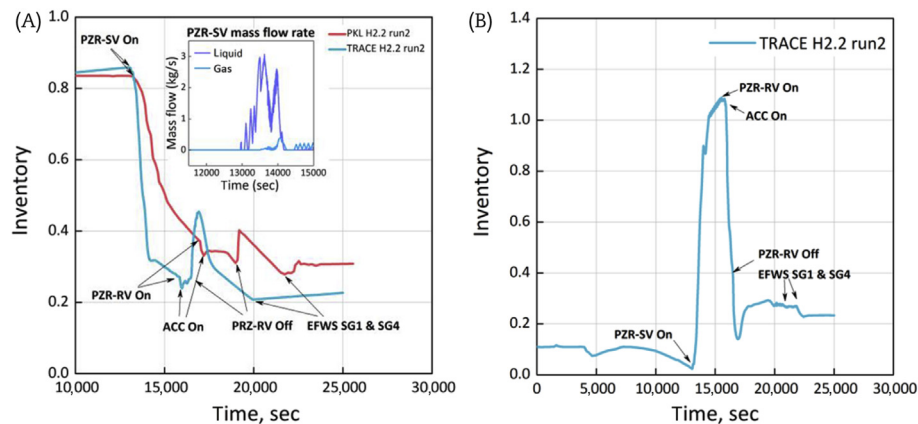

Fig. 12. Test H2.2 run 2. (A) Normalized primary inventory evolution in test H2.2 run 2. (B) Primary steam inventory evolution in test H2.2 run 2.
ACC, accumulator; EFWS, emergency feedwater system; PZR-RV, PZR relief valve; PZR-SV, PZR safety valve; SG, steam generator.

with the discrepancies observed for test H2.1. The overpredicted coolant loss via the PZR safety and RVs in the model, as shown by the steeper inventory drop in Fig. 12, again anticipated the first core uncovery and, thereafter, PCT excursion. This compensates for the previous time delay, and the core uncovery process started at the same time in both TRACE and PKL tests, at 16,800 seconds. Loop-seal clearing is induced by the next action, i.e., ACC injection, which resulted in complete core quench, as can be seen in both model and actual test results. In test H2.2 run 2, ACC injection is initiated at almost double the pressure of the previous tests. Compared to run 1, ACC discharge starts not only at a higher initial backpressure but also at a higher nitrogen pressure; therefore, ACC injection capability was higher, which enhanced the quenching effect in this case. Indeed, the ACC injection flow rate prevented a significant core heat up. Thus, the first PCT maximum resulting from test H2.2 run 2 was much lower than that observed in the two previous tests, an effect that the TRACE model was able to capture reasonably well despite the poor agreement in timing with test data (see Fig. 9). The ACCs in this test were sufficient to keep the core cooled for 4,150 seconds during the test (3,500 seconds in the model simulation) (Table 3).

Phase C started with the initiation of the next action, triggered by the second rise of CET, namely water feeding of SG1 and, 30 minute later, of SG4. The relatively larger feed flow rate, compared to the feed assumed in run 1, combined with the fact that the primary system was closed (PZR relief and safety valves closed after execution of PDE) proved sufficient to ensure constant cooling conditions and primary pressure reduction without the need for emergency primary feed, a behavior that the TRACE model was able to reproduce.

5. Conclusions

The main objective of this work was to assess the capabilities of the TRACE model to reproduce the timing and effects of the different AM actions under different boundary conditions and assumptions in the considered SBO scenarios (see Table 1). To ensure consistency of this validation exercise, the same TRACE nodalization has been applied to simulate all the three SBO tests without any attempt at adjusting model parameters to match the PKL tests data. The relevant processes and phenomena observed during these tests are described for each phase in the following subsections, with an emphasis on the evaluation of the performance of the simulation model during the corresponding phase.

5.1. Phase B

As for the first core heat up episode resulting from the water inventory loss through the PZR-SV, which began just before initiation of PDE, the modeled PCT excursions started earlier and at a slightly lower PV water level indication, compared to what the data showed. These discrepancies have been observed for both uniform and nonuniform radial (H2.2 run 2) power profiles in the core. As a result, while limitations in the current 1D model to capture 3D effects in the core and the upper plenum cannot be excluded, these observed discrepancies also hint at the need to represent more precisely the hydraulic volume distribution within the core and PV in the current model.

After initiation of PDE, an additional void is generated in the core and the rest of the primary system due to the fast depressurization. On the one hand, PDE causes water level swell in the core and induces higher flows due to suction effect from the PZR, which can slightly improve core cooling; however, the water mass inventory is further depleted. One can see in Fig. 9 that the TRACE model captured correctly these effects of PDE in the evolutions of PV water level and PCT (see in the figure the inflection of the overall increasing slope in temperature, particularly for test H2.1).

The start time of ACC injection in the CL is significantly affected by the discharge capacity of the PZR-RV. Thus the time difference from PDE initiation to start of ACC discharge is a good measure of the overall performance of the choked flow model in the presence of liquid entrainment at the PZR-RV. As can be seen in Fig. 9 for test H2.1, the model was able to reproduce well, qualitatively, this time interval; however, overall the model consistently overpredicted the discharge capacity across all three tests. This is more visible in Figs. 11 and 12 for the two other tests, which were characterized by a larger discharge capacity of the PZR-RV.

In H2.1, the amount of water injected into the CLs after opening the ACC valves was insufficient to completely quench the core, a peculiarity that the TRACE model could not reproduce. This discrepancy in behavior may be related to the modeling of steam condensation processes in the CLs at the ECC injection nozzles or/and some inaccuracies in the hydraulic volume distribution within the PV, as mentioned earlier. Impact of inaccurate condensation efficiency in the model could be amplified by the fact that a large amount of steam is present in the primary system at this stage, as shown in Figs. 10—12. This could therefore affect the loop seal clearing process and the amount of coolant transferred to the PV. As for test H2.2 run 1 and run 2, the TRACE model was able to reproduce the fact that ACC discharge was sufficient to quench the

Table 3
Chronology of all events in seconds.

	H2.1		H2.2 run 1		H2.2 run 2	
	PKL	TRACE	PKL	TRACE	PKL	TRACE
Conditioning phase						
SS FW shut-down	200	200	200	200	200	200
RCP shut-down	3,030	3,250	2,520	3,500	1,160	
SS FW activation (SG at 4 min)	5,220	4,660	4,610	5,250	1,350	1,350
Phase A & Start of the test (SOT): Shut-down of feedwater, PZR heater, and CVCS; start of core power decrease						
SDE	10,430	10,570	11,200	11,220	11,800	11,660
Primary pressure control via PZR-SV	12,160	11,680	12,230	12,300	13,040	12,960
Phase B						
PDE via PZR-RV	15,900	14,480	15,860	15,770	16,800	15,840
ACC injection	16,730	15,040	16,370	16,260	16,930	15,950
Phase C						
SS FW via mobile pump	20,000	17,500	18,650	19,350	20,050	21,600
SS FW shut-down	—	—	22,600	23,100	—	—
Primary side ECC injection	28,490	27,020	24,900	24,640	—	—

ACC, accumulator; CVCS, chemical and volume control system; ECC, emergency core coolant; FW, feed water; PDE, primary side depressurization; PKL, *Primärkreislauf-Versuchsanlage* (primary coolant loop test facility); PZR, pressurizer; PZR-RV, PZR relief valve; PZR-SV, PZR safety valve; RCP, reactor coolant pump; SDE, secondary side depressurization; SG, steam generator; SS, secondary side.

core. One could relate this to the larger PZR-RV discharge capacity at valve position 143 cm^2/145 and, for test H2.2 run 2, to the high nitrogen pressure in the ACCs.

The H2 tests provided a measure of further grace time before core heat up that ACC injection allows for, but long-term heat exchange between primary and secondary sides is necessary through at least one SG. This aspect of the system behavior has been captured well by the TRACE model. However, when the PZR-RV remained opened, as in tests H2.1 and H2.2 run 1, inventory continuously decreased, and third core uncovery occurred. The time difference between the second and third rises of PCT and CET in test H2.1 (H2.2 run 1) is 7,300 seconds (5,610 seconds) in the test and 8,825 seconds (4,910 seconds) in the TRACE model. The relatively large time differences between measurement and predictions reveal the importance of the modeling of the PZR relief and safety valve discharge capacity. In test H2.2 run 2, the PZR-RV was closed after completion of PDE. Therefore, inventory loss was stopped, and core heat up avoided.

5.2. Phase C

In tests H2.1 and H2.2 run 2, nitrogen was released from ACC into the RCS and later accumulated in the U-tubes of the SG's, thus affecting the heat sink between primary and secondary sides. However, the amount of water feed to the secondary side proved sufficient to establish heat exchange and keep the core quenched. This effect, in the presence of noncondensable gas, was captured by the TRACE model.

One can also recall for this phase of the scenario that the last AM action in tests H2.1 and H2.2 run 1 was to prevent low-pressure core heat up by primary injection via FPCP. Both experimental results and model predictions have shown a rapid core quench and sustainable long-term core cooling. In test H2.2 run 2, primary side injection proved unnecessary since the primary circuit was closed (PZR-RV closed after completion of PDE), a result that the TRACE model was able to reproduce.

5.3. Overall

In general, all relevant phenomena and AM actions observed during the H2 tests have been qualitatively reproduced by the TRACE model. A comparison to test data helped to reveal and correct for weak points of the original model, mainly about the modeling of heat losses and the behavior of the SGs and the ACC models when the water level reached the bottom of these components (through boil-off in the SG and discharge in the ACC).

One important conclusion from this work is that, in the case of long transients such as SBO scenarios and significant variation of the system temperatures, an accurate representation of dynamical heat losses is clearly necessary.

To achieve sufficient accuracy to investigate the issue of 3D behavior in the PV, the level of agreement with the H2 tests data obtained in this work will need to be further increased in the future. To do so, some improvements to the model will be necessary. In particular, the current multi-1D model of the PV will need to be replaced by a 3D VESSEL component available in TRACE. Moreover, the discrepancies observed at SOT can be further reduced by using available PKL data (both single phase and two-phase) to assess and revise the model for natural circulation conditions. Finally, the discharge capacity of the PZR safety and relief valves, and in particular their variation as a function of primary pressure and in the presence of liquid entrainment, will need to be further investigated for these tests.

Another important outcome of this work is related to the scaling of the TRACE results to a full-scale power plant, which is not considered in this work. Authors believe that this topic deserves separate consideration and publication, as is done, for example, in the TH analysis of other ITF facilities; see [17,19, and 20]. General overview of scaling approaches can be found in [21]. However, the main point is that all relevant phenomena observed and applied AM actions in PKL are expected also to occur in the real PWR NPPs; therefore, conclusions that are presented here are also applicable there. However, the fact that maximum operating pressure in the PKL facility does not exceed 50 bars makes all processes related to void formation and condensation faster compared to those processes in real PWRs. In the PKL facility, axial power profile is uniform along the PKL core; this means that the highest cladding temperatures occur at the top of the core region. In a PWR, however, due to axial nonuniformity, this is not the case.

Since the PKL facility has 1:1 elevation and 1:145 volume ratios to the reference PWR NPP, the surface to volume ratio of all vessel components in the PKL facility is larger than that of corresponding vessels in the reference PWR. Therefore, heat losses in the PKL facility are different from those in the reference PWR. In case of short transients, the heat loss effects can be smaller or negligible. However, when results for relatively long transient scenarios (like PKL SBO tests) are extrapolated to a real NPP, the dynamics of heat loss have to be taken into account, as was presented in Section 3.1.

A similar SBO experimental program was performed in the test facility ATLAS (Advanced Test Loop for Accident Simulation), which simulates an APR1400 (Advanced Power Reactor 1,400 MWt) [18]. Results of heat loss analysis here are in line with the conclusions obtained in the ATLAS model [17]. As was shown there, heat losses have a large effect on the SBO transient. On the other hand, results for APR1400 have shown a negligible effect of heat loss on the SBO transient.

Conflicts of interest

All authors have no conflicts of interest to declare.

Acknowledgments

Nomenclature

ACC	Accumulator
AM	Accident management
CET	Core exit temperature
CL	Cold leg
CVCS	Chemical/volume control system
DC	Downcomer
DCT	Downcomer tube/pipe
DCV	Downcomer vessel
ECC	Emergency core coolant
ECCI	Emergency core coolant injection
ECCS	Emergency core cooling systems
EFWS	Emergency feedwater system
EOT	End of test
eRHR	Emergency residual heat removal
FPCP	Fuel pool cooling pump
HL	Hot leg
HPSI	High-pressure safety injection
HTC	Heat transfer coefficient
ITF	Integral Test Facility
LPSI	Low-pressure safety injection, also

LHSI	low head safety injection
LS	Loop seal
MSRCV	Main-steam relief control valve
MSRV	Main steam relief valve
NEA	Nuclear Energy Agency
OECD	Organization for Economic Cooperation and Development
PCT	Peak (heater-rod) cladding temperature
PDE	Primary-side depressurization
PKL	Test facility, (German acronym for "Primärkreislauf", means: primary circuit, RCS)
PZR	Pressurizer
PS	Pump seal, cross-over leg
PV	Pressure vessel
RCP	Reactor coolant pump
RCS	Reactor cooling system
RV	Relief valve
SBO	Station blackout
SDE	Secondary side depressurization
SOT	Start of test
SG	Steam generator
SS	Secondary side
SV	Safety valve
UH	Upper head

Appendix A. Supplementary data

Supplementary data related to this article can be found at https://doi.org/10.1016/j.net.2017.12.005.

References

[1] I. Tóth, R. Prior, O. Sandervag, K. Umminger, H. Nakamura, N. Muellner, J.R. Alonso, Core exit temperature (CET) effectiveness in accident management of nuclear power reactors, in: Committee on the Safety of Nuclear Installations, OECD, Nuclear Energy Agency, 2010.

[2] J. Freixa, V. Martínez-Quiroga, O. Zerkak, F. Reventós, Modelling guidelines for core exit temperature simulations with system codes, Nuclear Eng. Design 286 (2015) 116—129.

[3] Division of Risk Assessment and Special Projects. Office of Nuclear Regulatory Research, TRACE V5.840 Theory Manual - Field Equations, Solution Methods, and Physical Models, U.S. Nuclear Regulatory Commission, 2013.

[4] Paul Scherrer Institute, Steady-state and Transient Analysis Research of the Swiss Reactors (STARS Project), 2011. https://stars.web.psi.ch.

[5] K. Umminger, L. Dennhardt, S. Schollenberger, B. Schoen, Integral test facility PKL: experimental PWR accident investigation, Sci. Technol. Nuclear Install. 2012 (2012).

[6] K. Umminger, B. Brand, W. Kastner, The PKL test facility of framatome ANP-25 years experimental accident investigation for Pressurized Water Reactors, VGB PowerTech 1 (1) (2002) 36—42.

[7] K. Umminger, T. Mull, B. Brand, Integral effect tests in the PKL facility with international participation, Nuclear Eng. Technol. 41 (6) (2009) 765—774.

[8] K. Umminger, T. Mull, B. Brand, Integralversuche in der PKL-anlage mit internationaler Beteiligung, Atw. Int. Z. Kernenerg. 55 (3) (2010).

[9] AREVA NP, Pressurized Water Reactor Integral System Test Facility −PKL, official web page: http://de.areva.com/EN/customer-819/pkl-pwr-integral-system-test-facility.html (September 2017).

[10] J. Freixa, SBLOCA with Boron Dilution in Pressurized Water Reactors, Impact to the Operation and Safety, PhD Thesis, Technical University of Catalonia, 2008.

[11] S.P. Schollenberger, Determination of Heat Losses in the PKL Test Facility, 2nd edition (1990−2015), May 2016. Technical Report, PTCTP-G/2016/en/0019, Erlangen, Germany.

[12] I. Clifford, O. Zerkak, A. Pautz, H. Yao, J. Freixa, System Code Validation Series Based on a Consistent Plant Nodalisation of the ROSA/LSTF Integral Test Facility Using TRACE v5.0 Patch 4, NUTHOS-11, Gyeongju, Korea, October 9−13, 2016.

[13] J. Freixa, A. Manera, Analysis of an RPV upper head SBLOCA at the ROSA facility using TRACE, Nuclear Eng. Design 240 (7) (2010) 1779−1788.

[14] A.B. Salah, J. Vlassenbroeck, H. Austregesilo, Experimental and analytical assessment of natural circulation interruption phenomenon in the LSTF and PKL test facilities, Nuclear Technol. 192 (1) (2015) 1−10.

[15] B.A. Salah, J. Vlassenbroeck, CATHARE assessment of natural circulation in the PKL test facility during asymmetric cooldown transients, Sci. Technol. Nuclear Install. 2012 (2011).

[16] USNRC, TRACE Pressurized Water Reactor Modeling Guidance, 2012. Technical Report.

[17] X. Yu, H. Park, Y. Kim, K. Kang, S. Cho, K. Choi, Systematic analysis of a station blackout scenario for APR1400 with test facility ATLAS and MARS code from scaling viewpoint, Nuclear Eng. Design 259 (2013) 205−220.

[18] Yeon-Sik Kim, Xin-Guo Yu, Kyoung-Ho Kang, Hyun-Sik Park, Seok Cho, Ki-Yong Choi, Analysis of a station blackout scenario with an atlas test, Nuclear Eng. Technol. 45 (2) (2013) 179−190.

[19] J. Freixa, V. Martínez-Quiroga, F. Reventós, Qualification of a full plant nodalization for the prediction of the core exit temperature through a scaling methodology, Nuclear Eng. Design 308 (2016) 115−132.

[20] J. Freixa, A. Manera, Verification of a TRACE EPR™ model on the basis of a scaling calculation of an SBLOCA ROSA test, Nuclear Eng. Design 241 (3) (2011) 888−896.

[21] M. Ishii, S.T. Revankar, T. Leonardi, R. Dowlati, M.L. Bertodano, I. Babelli, W. Wang, H. Pokharna, V.H. Ransom, R. Viskanta, J.T. Han, The three-level scaling approach with application to the Purdue University Multi-Dimensional Integral Test Assembly (PUMA), Nuclear Eng. Design 186 (1−2) (1998) 177−211.